



# Approach to Obtain Electrospun Hydrophilic Fibers and Prevent Fiber Necking

Thorsten Fischer, Martin Möller,\* and Smriti Singh\*

Solution electrospinning of a blend containing a hydrophobic polymer with a hydrophilic functional polymer as an additive is a simple and straightforward route to obtain functional and hydrophilic fibers accompanied by the mechanical properties of the hydrophobic polymer. However, this process of thermodynamically unfavored surface segregation of the hydrophilic additive is not well understood. To understand the process the dependencies of the surface hydrophilization on type of hydrophilic polymers, the solvent, and the process, using poly(caprolactone) (PCL) as the matrix polymer is explored. The results show that hydrophilic fibers can be obtained using different additive hydrophilic polymers. The combination of polymer blends which show this effect can be predicted using the Flory–Huggins interaction parameter. In addition mechanical and micromechanical properties of PCL fibers blended with NCO-terminated star-shaped poly(ethylene glycol) (sPEG-NCO) as additive are investigated. In this context blending with sPEG-NCO turns out to be a powerful tool to prevent fiber necking rendering this method an interesting candidate for tissue engineering application, where it is mandatory to retain the surface properties under mechanical stress.

(plasma treatment, hydrolysis), reduced pore size and multi-steps (grafting, layer-by-layer), or the need of a special setup (co-axial spinning). In contrast to these methods, polymer blending is a facile and single-step approach.<sup>[1,8]</sup> For instance Grafahrend et al. used this single step modification method for fabrication of degradable scaffold using of poly(D,L-lactide-co-glycolide) (PLGA) with NCO-terminated star-shaped poly(ethylene glycol) (sPEG-NCO) for its application as hernia mesh. The mesh was investigated by X-ray photoelectron spectroscopy (XPS) which indicated sPEG-NCO on the shell. Consequently, the water contact angle drops from 120° for pure PLGA meshes to 0° (complete wetting). Similarly, Planz et al. electrospun a blend of poly(caprolactone) (PCL) with gelatin. In this case the contact angle drops from 119° for the pure PCL fibers to 0° for the blended fibers. Thus using functional hydrophilic polymers,

## 1. Introduction

Electrospinning is a versatile method to produce fibers with a high surface area. Hydrophilic electrospun fiber meshes can be used for several applications like scaffolds for tissue engineering or as separation or filtration membranes. To enhance the wettability of the electrospun fibers and to tailor its hydrophilicity widely used methods include plasma treatment, surface hydrolysis, grafting, layer-by-layer assembly on the surface of fibers, co-axial spinning, and spinning of hydrophilic and hydrophobic polymer blends.<sup>[1–7]</sup> Most of these methods suffer from inherent drawbacks such as homogeneity and stability

this method can be used for in situ integration of bioactive components like cell recognition sequences in one step. However, the understanding of this thermodynamically unfavored process remains a major challenge to establish this method as a standard for making hydrophilic fibers. In general, on electrospinning of blended polymers, the polymer with the lower surface energy will tend to cover the surface. This was for example shown by Hardman et al. in a system containing poly(styrene) (PS) as matrix polymer and fluoroalkyl end-functionalized PS as additive. The water contact angle in this system increases from 120° for pure PS to 150°.<sup>[9]</sup> While for fibers obtained from PCL and NCO-PEG blends, this effect was explained due to the enhancement of charge shielding by the NCO-groups hydrolyzing to the amine. During the electrospinning process, the charge density increases especially on the fiber surface. These charges are shielded more efficiently in a medium of a higher permittivity leading to electrostatic driven surface segregation.<sup>[1]</sup> Contrary, Zhang et al.<sup>[10]</sup> deduced this surface segregation phenomenon in their PEO/chitosan system as a solvent effect, where phase separation occurs falling down the binodal curve during solvent evaporation, which means there is an occurring miscibility gap reaching a certain temperature.

Moreover, it remains unclear how the surface coverage of the additive hydrophilic polymer behaves under mechanical stress during handling or fabrication of the sample or for mechano-sensitive tissue engineering application. It is well known that semi-crystalline polymer fibers like PCL,

T. Fischer, Prof. M. Möller, Dr. S. Singh  
 DWI—Leibniz-Institute for Interactive Materials e.V.  
 Forckenbeckstr. 50, 52056 Aachen, Germany  
 E-mail: moeller@dwirwth-aachen.de; singh@dwirwth-aachen.de

Prof. M. Möller  
 Institute for Technical and Macromolecular Chemistry RWTH Aachen  
 Worringer Weg 1, 52056 Aachen, Germany

The ORCID identification number(s) for the author(s) of this article can be found under <https://doi.org/10.1002/mame.201900565>.

© 2019 The Authors. Published by WILEY-VCH Verlag GmbH & Co. KGaA, Weinheim. This is an open access article under the terms of the Creative Commons Attribution License, which permits use, distribution and reproduction in any medium, provided the original work is properly cited.

DOI: 10.1002/mame.201900565

poly(methyl methacrylate) (PMMA) show necking when subjected at strain ratios as low as 8%.<sup>[11]</sup> Fiber necking is a cold crystallization process caused by local molecular alignment. Consequently, the microenvironment of the necked parts alters dramatically in stiffness, crystallinity, and topography. This, in turn, can directly affect the properties of the fiber. There are numerous studies where electrospun fibers are used as scaffold<sup>[12–17]</sup>; however, the phenomenon of necking in such cases has been widely overlooked. Necking can occur unintended while handling like during the use of a rotating mandrel for the production aligned fibers<sup>[18]</sup> or using the fleece as basement membrane mimic for establishing in vitro models like lung,<sup>[13]</sup> blood vessel,<sup>[19]</sup> renal,<sup>[20]</sup> or skin tissue,<sup>[21]</sup> where the membrane is expected to experience mechanical forces to replicate the physiological conditions.

In this work, we systematically explore the process of hydrophilization by surface segregation on blending. We choose PCL as matrix polymer due to its good mechanical stability and biodegradability.<sup>[22]</sup> On the one hand, we canvass the argumentation of permittivity and charge shielding by varying the solvent, the functional group, and the need for electrostatic interaction itself with the help of forcespinning method. On the other hand we investigate the argumentation of an occurring miscibility gap by varying the additive polymer, that is, OH-terminated star-shaped poly(ethylene glycol-co-propylene glycol) (sPEG-OH), poly(glycerol sebacate) (PGS), poly(2-hydroxyethylmethacrylate) (PHEMA), poly(ethylene imine) (PEI), and poly(*N*-isopropylacrylamide) (PNIPAm), determining the surface enrichment by XPS, and applying Flory–Huggins polymer miscibility theory. Furthermore, we highlight the potential, which arises from this method using sPEG-NCO, by investigating the mechanical and micromechanical properties of blended and non-blended fibers using tensile testing within the SEM chamber.

## 2. Experimental Section

### 2.1. Materials

PCL 80 kDa, polyacrylic acid (PAA) 1.2 kDa and 100 kDa, PEI (0.8 kDa), PNIPAm (10 kDa), PHEMA (20 kDa), dextran (40 kDa), acetone, dimethylsulfoxide (DMSO), dimethylformamide (DMF), formic acid (FA), methyl formate, toluene, glycerol, sebacic acid, and trifluoroacetic acid (TFA) were purchased from Sigma-Aldrich. Chloroform, tetrahydrofuran (THF), methanol, and dried acetone were purchased from VWR. All chemicals were used as received without any purification. Star shaped OH-poly(ethylene glycol)<sub>80</sub>-stat-poly(propylene glycol)<sub>20</sub>,  $M_w = 12$  kDa) (sPEG-OH) was procured from CPT GmbH and functionalized with isocyanate groups (sPEG-NCO) as previously reported.<sup>[1]</sup>

### 2.2. Synthesis of Poly(Glycerol-Sebacate)

Poly(glycerol-sebacate) (PGS) was synthesized as reported by Wang et al.<sup>[23]</sup> Briefly, 0.2 mol glycerol and 0.2 mol sebacic acid were kept under nitrogen atmosphere at 120 °C for 24 h to initiate polycondensation. After that, the pressure was reduced to 10<sup>-4</sup> mbar for another 48 h at 120 °C. The polymer

was characterized by NMR and gel permeation chromatography (GPC).

### 2.3. Electrospinning

Unless otherwise noted a typical spinning solution consists of 15 wt% of PCL in CHCl<sub>3</sub>/CH<sub>3</sub>OH (75 vol% CHCl<sub>3</sub>, 25 vol% CH<sub>3</sub>OH). For the production of blended fibers, 2 wt% of the additive polymer was dissolved in 50 μL of acetone in case of sPEG-NCO/-OH 50 μL of THF in case of PGS. 10 μL of acidic water (0.118 mol L<sup>-1</sup> TFA in water) was added to improve conductivity.<sup>[1]</sup> The solutions were mixed together directly before spinning and spun with a collector-to-needle distance of 15 cm, an applied voltage of 20 kV ± 2 kV, and a syringe pump speed of 1 mL h<sup>-1</sup>. FITC-collagen labeled fibers were electrospun using following spinning conditions: FITC-collagen was taken 0.5 wt% to sPEG-NCO and premixed with the sPEG-NCO for 120 min. The labeled 2 wt% sPEG-NCO was added to 15 wt% PCL in CHCl<sub>3</sub>: acetone (3:1) and spinning was performed as the abovementioned spinning parameters.

### 2.4. Centrifugal Force Spinning

Centrifugal force spinning was carried out in a CyclOne L1000 (FibeRio, United States) with 4000 rpm and a 27-gauge flat-tipped needle. 15 wt% of PCL with 2 wt% of sPEG-NCO as an additive in a mixture of 75 vol% CHCl<sub>3</sub> and 25 vol% CH<sub>3</sub>OH was used.

### 2.5. Fiber Characterization

Scanning electron microscopy (SEM) was performed with a Hitachi S3000 N and/or Hitachi S 4800 (Hitachi, Japan) with acceleration voltages between 1 and 20 kV. To improve the conductivity a 10 nm layer of gold/palladium (80:20) was sputter coated on the fiber meshes, using an ACE 600 sputter coater (Leica, Germany). Image analysis was performed with ImageJ analysis software. Fluorescence microscopy was performed with a Zeiss Axioplan 2 (Zeiss, Germany).

Water contact angle measurements were performed with a G2 contact angle measuring system (Krüss, Germany) with a drop volume of 3 μL.

X-ray photoelectron spectroscopy (XPS) was performed with a Kratos Ultra Axis (Kratos, United Kingdom). The samples were excited with monochromatic Al-K<sub>α1,2</sub> radiation (1486.6 eV). The resulting spectra were analyzed with CasaXPS software (Casa Software Ltd., United Kingdom).

Tensile tests were performed with a tensile tester (Zwick Roell, Germany). The strain rate was set to 0.01 Hz to determine the elastic modulus and the maximum strain and to 0.01 or 0.25 Hz to determine the energy loss and the creep in a cyclic test. The meshes were stretched to 15%, which mimics the maximum stretching of the alveoli during breathing.<sup>[24]</sup> For estimation of the energy loss, the loading and unloading cycles were fitted with Equation (1) (except the first loading cycle, where a third order polynomial fit was used) with  $\gamma_0$ ,  $A$ , and  $R_0$  being arbitrary fitting parameters and integrals were divided.

$$f(x) = y_0 + A \cdot e^{R_0 \cdot x} \quad (1)$$

The creep is defined as the first point, where the unloading curve is equal to the set pre-force. Twenty cycles were performed taking an average from three meshes.

The failing mechanisms and nature of the creep were investigated with a Microtest 200 N (Deben, United Kingdom) inside a Hitachi S3000 N. The strain rate was set to 1.5 mm min<sup>-1</sup> with a grip-to-grip separation of 10 mm.

Small angle X-ray scattering (SAXS) was performed in an Empyrean X-ray diffractometer (PANalatical, Germany) in transmission. The angle  $\theta$  was transformed into the scattering vector  $q$  with Equation (2).

$$q = \frac{4\pi}{\lambda_K} \sin \frac{2\theta\pi}{360^\circ} \quad (2)$$

with  $\lambda_K$  being the  $K_\alpha$ -radiation of the copper source (0.1542 nm). The background was measured separately and subsequently subtracted. To determine the crystallinity the area of the crystalline domain was divided by the complete area using the method of van den Burght.

### 3. Results and Discussion

Pure PCL and PCL with sPEG-OH (mass ratio: 88 wt% PCL and 12 wt% sPEG-OH) were electrospun and compared to verify the surface segregation (see the Experimental Section for details). In both cases, homogeneous fibers were spun (Figure 1a,b) with a comparable fiber diameter (Figure 1c, average diameter PCL: 1.94  $\mu$ m, average diameter PCL+sPEG-OH: 2.23  $\mu$ m). Furthermore, the contact angle drops down to 0° with sPEG-OH as additive, which implies that the surface is covered by sPEG-OH. This

is a counter-intuitive result, because in general the moiety with the lower surface energy, which is the hydrophobic one, will tend to segregate to the surface. When PCL is blended with sPEG-OH as additive, the surface energy of the additive is higher than the surface energy of the PCL, thus in thermodynamic equilibrium, the additive should tend to be buried inside the PCL matrix to reduce the energy of the system. This is not the case, which indicates that the electrospinning process adds a kinetic component to the thermodynamic aspect that normally defines polymer mixing; leading to the process of surface segregation. To approach the thermodynamic equilibrium fiber meshes of PCL and sPEG-OH were heated up to 55 °C, which is just below the melting temperature of PCL. However, heating did not change the surface hydrophilicity. We presume that this could be due to the energy barrier that is too high to be overcome at this temperature. With further heating to 80 °C, the fibers were completely molten and the contact angle rose to 60°, which is similar to a solvent cast film of PCL+sPEG-OH implying the metastability of surface segregation process (Figure S1, Supporting Information).

The kinetically driven process of surface segregation was previously explained by the presence of polar groups (urethane, urea, amine, etc.) associated with additive polymers which can act as charge carriers.<sup>[1,25-27]</sup> Polar groups during electrospinning can result in the enhancement of charge shielding and drive the surface segregation of the additive.<sup>[1]</sup> This can further be influenced by the use of solvents with different permittivity. To probe the influence of the solvents and the permittivity we chose solvents with low (chloroform, THF) and high (acetone) permittivity, and with low (chloroform, acetone) and high (THF) conductivity, respectively (Table S1, Supporting Information). Furthermore to investigate the influence of the functional group we use NCO and OH terminated sPEG of the same molecular weight. For all the meshes 15 wt% of PCL was used while sPEG-NCO or sPEG-OH was kept to 2 wt% (mass ratio 88% PCL to 12% sPEG).

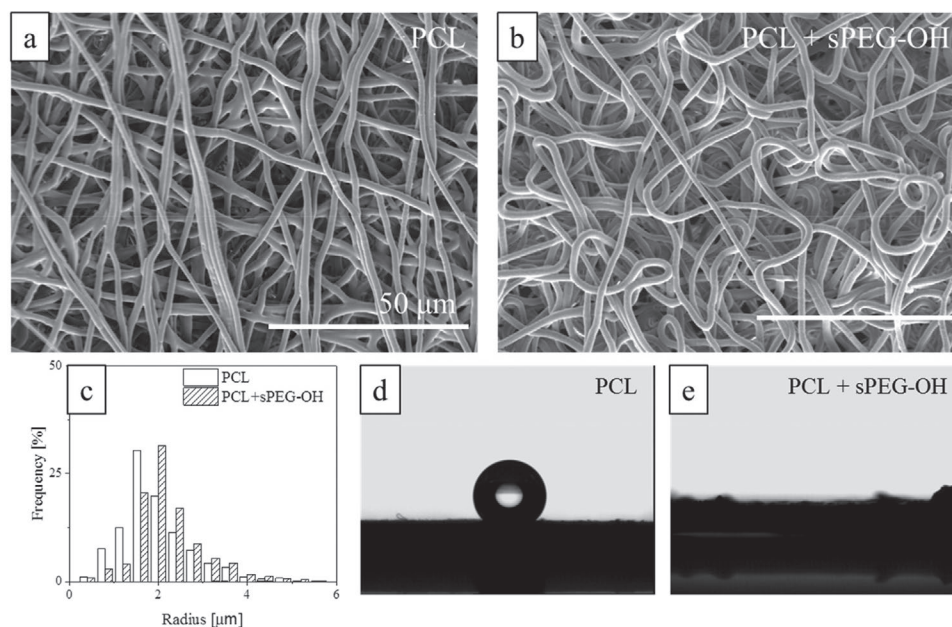


**Figure 1.** SEM image of electrospun fibers composed of a) PCL, b) PCL with sPEG-OH as an additive, c) their respective fiber diameter distribution and d) the respective contact angle of these fibers for PCL, and e) PCL with sPEG-OH as additive.

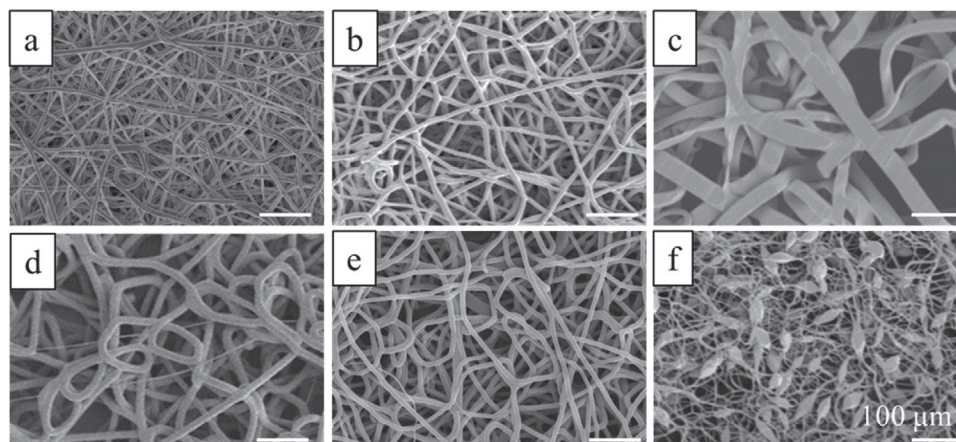


**Figure 2.** SEM image of electrospun PCL fibers with a–c) sPEG-NCO and d–f) sPEG-OH as additive with (a,d) CHCl<sub>3</sub>, (b,e) THF, and (c,f) acetone as solvent.

In case of sPEG-NCO, the isocyanate group will react with the humidity to amine-groups, which itself will crosslink with isocyanate groups forming a hydrogel layer at the surface.

Irrespective of the solvent property and PEG functionality the meshes obtained were hydrophilic in nature. However, as expected solvent influenced the fiber morphology. Though chloroform and THF as a solvent for sPEG-OH and sPEG-NCO did not influence the fiber morphology (Figure 2a,b,d,e), a clear difference in fiber morphology was observed with acetone as a solvent (Figure 1c,f). With acetone sPEG-NCO as an additive resulted in flat ribbon shaped fibers while sPEG-OH formed fibers with beaded morphology. The mean size of flat fibers obtained with sPEG-NCO was  $7.1 \pm 1.3 \mu\text{m}$ , and the ratio of axial diameters corresponded to 4.5 which suggests that the fiber surface is significantly enhanced compared to beaded fibers. This occurs most likely due to rapid precipitation of PCL in acetone on electrospinning and fast self-crosslinking of sPEG-NCO forming a thin skin. As the solvent evaporates the skin collapses leading to the formation of ribbon-like fibers,<sup>[28]</sup> while this was not the case with sPEG-OH as additive. Nevertheless, the hydrophilicity of the meshes was independent of the polarity of the PEGs. From these data, it is clear that surface segregation of the additive polymer takes place irrespective of the functionality and only the fiber morphology is affected by the presence of fast reacting isocyanate group.

Additionally, the hypothesis of the permittivity of the driving force for the surface segregation can be verified with a spinning process, which does not rely on electrostatic interaction. Therefore, we apply for spinning to fabricate fibers, which uses centrifugal force rather than electrostatic force as in the electrospinning. In this process, the geometry and morphology of the microfibers are controlled by the rotational speed of the spinneret, collection system, and temperature and the fibers are collected circumferential to the spinneret. Forcespinning and electrospinning process both exhibit fast solvent evaporation and high aspect ratios of the fibers. The PCL + sPEG-NCO fiber mesh obtained by forcespinning showed complete wetting on contact angle measurement (Figure S2, Supporting Information). From this, we can deduce that applied voltage and conductivity does not play a role in surface segregation.

During electrospinning, the kinetics of phase separation is enhanced by drop in temperature due to fast solvent evaporation which in turn depends on the evaporation rate, solvent quality, and concentration.<sup>[29]</sup> The fast solvent evaporation possibly leads to the spinodal decomposition of polymer blends which is solely driven by diffusion. PCL and PEG-OH which are thermodynamically miscible at room temperature upon electrospinning phase separate due to fast solvent evaporation following the argumentation of Zhang et al.<sup>[10]</sup> PCL which is higher in concentration gets kinetically frozen by the change in viscosity upon reduction in solvent fraction while PEG which is well miscible with PCL diffuses out with the solvent. Thus the PCL-rich phase forms the matrix, whereas the shell is formed from the PCL poor phase, that is, the sPEG-NCO or PEG-OH. To confirm this hypothesis and to investigate the versatility of this method the additive polymers were varied. Table 1 shows different additive polymers and spinning conditions with PCL as a matrix polymer.

With sPEG-NCO, sPEG-OH, linear PEG, and poly(glycerol sebacate) (PGS), poly(2-hydroxyethylmethacrylate) (PHEMA), poly(ethylene imine) (PEI), and poly(*N*-isopropylacrylamide) (PNIPAm) hydrophilic fibers were obtained, whereas with

**Table 1.** Dependence of the additive polymer on the surface segregation.

Additive polymer	Solvent	$M_w$ [kDa]	Surface segregation	U [kV]	D [cm]	V [ $\text{mL h}^{-1}$ ]
sPEG-NCO	Acetone	12	✓	20	15	1.0
sPEG-OH	Acetone	12	✓	20	15	1.0
Linear PEG	Acetone	40	✓	20	20	1.2
PGS	THF	2-3	✓	19	15	2.0
PHEMA	Acetone	20	✓	22	15	1.0
PEI	Chloroform	0.8	✓	22	15	1.5
PNIPAm	Chloroform	10	✓	20	15	2
PVP	Chloroform	55	×	24	15	0.5

$M_w$ , Molecular weight; U, Applied voltage; d, Collector-to-needle distance; v, Syringe pump speed; mass fraction ratio of hydrophobic to hydrophilic polymer (88%:12%).

**Table 2.** Molar volume and molar attraction constants.

Group	Molar volume [cm <sup>3</sup> mol <sup>-1</sup> ]	Molar attraction constant [(J cm <sup>-3</sup> ) <sup>0.5</sup> ]
–CH <sub>3</sub> –	31.8	446
–CH <sub>2</sub> –	16.5	270
–CH–	1.9	47
–O–	5.1	194
–CO–	10.7	536
–COO–	19.6	609
–N–	–5	–6.1
–NH–	8.5	293
–NH <sub>2</sub>	18.6	562
–N–CO–	5.7	529

Adapted from ref. [31].

poly(vinyl pyrrolidone) (PVP) fibers remain hydrophobic with contact angles close to pure PCL fibers (Table S2, Supporting Information). This shows that for the different PEGs, PGS, PHEMA, PEI, and PNIPAm surface segregation occurs, whereas in the case of PVP the fiber surface is covered predominantly by PCL.

In order to trace the limits of surface segregation as in case of PVP and PCL blend, we applied a theoretical approach based on Flory–Huggins interaction which expresses thermodynamic properties of polymer solutions and blends in terms of the polymer-solvent interaction. The miscibility of the polymers is considered by the Flory–Huggins interaction parameter  $\chi$ , which can be estimated from Equation (3).

$$\chi_{AB} = \frac{V_{\text{ref}}(\delta_A - \delta_B)^2}{RT} \quad (3)$$

where  $V_{\text{ref}}$  is a “reference volume,” which is usually assumed to be 100 cm<sup>3</sup> mol<sup>-1</sup>,<sup>[30]</sup>  $\delta$  the respective Hildebrand solubility parameter,  $R$  the gas constant, and  $T$  the temperature. The Hildebrand solubility parameter is defined as

$$\delta = \frac{\sum F_i}{V_M} \quad (4)$$

with  $F_i$  being the sum of the molar attraction constants and  $V_M$  the molecular weight of one repeating unit.<sup>[30]</sup> The molar attraction constants and the molar volume can be estimated by the summation of the single groups of one repeating unit with values reported from Coleman et al. (Table 2).<sup>[31]</sup> In general a  $\chi$ -parameter greater than 0.5 means unlike interaction between blends, between 0 and 0.5 a weak, and below 0 a strong interaction. For simplification linear PEG instead of sPEG-NCO or sPEG-OH was used for the calculation. The  $\chi$ -parameter for PEG and PCL was calculated as  $\approx 0$  at 25 °C, which means, the polymers show good miscibility at room temperature. For PNIPAm and PEI, the  $\chi$ -parameter was calculated from Equation (1) to be 0.04 and 0.08, respectively, indicating still good miscibility. For PVP the  $\chi$ -parameter was found to be 1.05, which means a very unlike interaction. Thus,

**Table 3.** Atomic concentration calculated from XPS of PCL fibers and PCL with different additive polymers.

Polymer		Atomic concentration [%]		
		C	O	N
PCL	Theoretical	75.0	25.0	0
	Experimental	78.6	21.4	0
PCL+sPEG-NCO	Theoretical	74.2	25.7	0.1
	Pure sPEG-NCO	68.2	31	0.7
PCL+PEI	Experimental	72.7	26.8	0.6
	Theoretical	74.0	22.0	4.0
PCL+PNIPAM	Pure PEI	66.7	0	33.3
	Experimental	72.8	24.1	3.1
PCL+PNIPAM	Theoretical	75	23.5	1.5
	Pure PNIPAM	75	12.5	12.5
	Experimental	75.9	20.0	4.2

the non-miscibility of polymer blends hinders and prevents the hydrophilic component to surface segregate. A theoretical consideration of the  $\chi$ -parameter with PHEMA might be interesting, but there are no values for the molar attractions constants of alcohols or acids reported as the strong associative nature of these groups leads to a high inherent error.<sup>[31]</sup>

XPS was used to quantify the surface enrichment of the hydrophilic polymer (Table 3). For the calculation of the surface segregation, the nitrogen content of the blend was calculated and compared to the pure additive polymer. PCL+sPEG-NCO fibers, which possess the lowest  $\chi$ -parameter, exhibit nearly complete segregation of the sPEG-NCO (nitrogen content in the blend: 0.6%, within pure sPEG-NCO: 0.7%). In general, the  $\chi$ -parameter seems to reflect the surface segregation of the additive polymer and can, therefore, be used to predict the behavior of fibers. With increasing  $\chi$ -parameter (sPEG-NCO < PNIPAm < PEI) the surface enrichment, that is, the experimental atomic nitrogen concentration divided by the nitrogen content of the pure compound, decreases (sPEG-NCO: 85.7%, PNIPAM: 33.6%, PEI 9%).

Further, we used FITC labeled collagen I to visualize the phase separation. The labeled protein was pre-mixed with sPEG-NCO prior to electrospinning for 120 min. This provided enough time for the chemical crosslinking of the amine group of collagen to the sPEG-NCO but still preventing the complete hydrolysis or self-gelation of sPEG-NCO (Scheme S1, Supporting Information). Collagen itself is largely hydrophobic in nature but when it is covalently linked to the sPEG-NCO, the protein is driven along on the surface. Due to the thickness of the fibers, in this case, the FITC-collagen I could be visualized using fluorescence microscopy (Figure S3, Supporting Information).

With respect to the use of electrospun fibers for tissue engineering, the use of sPEG-NCO as an additive for blending has an edge over the other above used polymers blends. On the one hand, it provides a stable hydrophilic surface and on the other the isocyanate self-crosslink to form a thin hydrogel film on fiber surface or can couple with NH<sub>2</sub>/SH groups of the peptides/proteins for biofunctionalization (Scheme S1, Supporting Information). Therefore, we choose sPEG-NCO as an additive

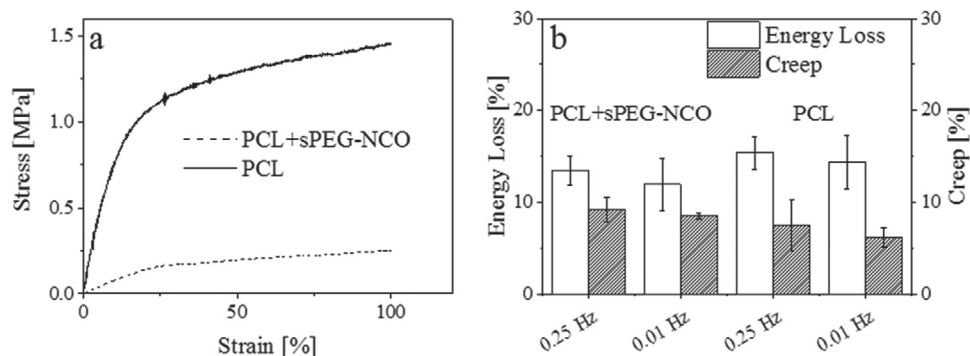


**Figure 3.** a) Stress–strain curve of PCL and sPEG-NCO fibers and b) energy loss and creep after the 20th cycle for PCL and PCL+sPEG-NCO fibers. sPEG-NCO as additive renders the mesh more elastic. Along with a higher modulus, the pure PCL fibers show also a slightly higher energy loss.

polymer to further investigate the impact of blending on the mechanical and micromechanical properties compared to pure PCL fibers. Using uniaxial tensile tests the elastic modulus of PCL fibers was calculated to be 9.0 MPa, which is similar to literature values (8.4 MPa)<sup>[32]</sup> whereas, a threefold reduction in elastic modulus of fibers with sPEG-NCO as additive was obtained. The elastic modulus of sPEG-NCO fibers was 2.7 MPa (Figure 3a). This reduction is caused by the amorphous nature of sPEG-NCO which is in the mass ratio of 12% to PCL.

The micromechanical of electrospun fibers can affect cell behavior. Therefore to elucidate the micromechanical properties and failure mechanisms, cyclic tensile tests and in situ tensile testing within a scanning electron microscopy (SEM) chamber was performed. The failure mechanisms can cover structural changes on the microscopic level such as fiber necking and on the macroscopic level such as fiber alignment. Fiber necking is a cold crystallization process as it leads to a molecular orientation within the fiber along with a decrease of the fiber diameter. Since physiological strains on the electrospun fleece, for instance, used as basement membrane mimic in an in vitro lung model, can reach up to 15%, this value was chosen as a setpoint (Figure S4, Supporting Information).<sup>[13,24]</sup> Cyclic measurements were performed at 0.25 Hz to mimic breathing and for comparison at 0.01 Hz. Energy-loss, which is the amount of dissipated energy, and creep, which is caused by the irreversible

structural changes mentioned above, was calculated after the 20th cycle (Figure 3b; Figures S5 and S6, Supporting Information). However, no dependence on the strain rate was found. The energy loss was slightly higher for PCL fibers, which reflects the higher modulus. Both PCL and PCL+sPEG-NCO meshes exhibit a comparable creep. To trace whether the creep is caused by fiber alignment or necking in situ tensile testing was performed in the SEM with online imaging and measuring of tensile property. The stretching of the mesh was stopped at defined strain ratios to investigate the structural changes. The stress–strain curves of these measurements exhibit a stress-relaxation at the strain ratio, where the measurement was halted (Figure S7, Supporting Information). Stress relaxation is known for polymers, which exhibits a viscoelastic behavior such as amorphous, semicrystalline, or biopolymers.<sup>[11]</sup>

The SEM images which were subjected to 0%, 15%, and 100% strain are shown in Figure 4. At 15% strain, necking is more pronounced for the PCL fibers. Further stretching to 100% causes necking at multiple points and fiber to tend to align. With sPEG-NCO necking is significantly reduced and fiber alignment is more prominent (Figure S8, Supporting Information). Since these fibers are softer, alignment is facilitated.<sup>[33]</sup> Furthermore, it was observed that the thin hydrogel layer covering the fiber surface can maintain the surface properties even if the PCL core is necked.

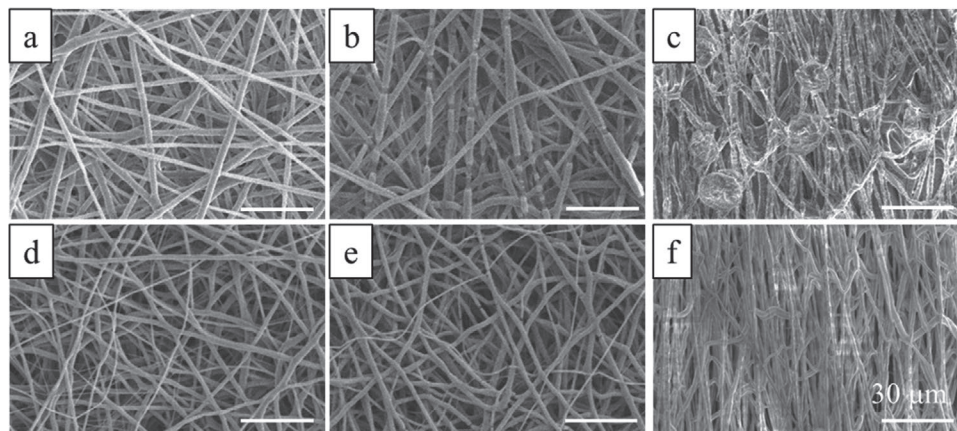


**Figure 4.** SEM images of a–c) PCL, and d–f) PCL+sPEG-NCO fibers. a, d) 0% strain, b, e) 15% strain, c, f) 100% strain. Fiber necking is more pronounced for pure PCL fibers, whereas fibers with sPEG-NCO as additive have a more pronounced alignment.

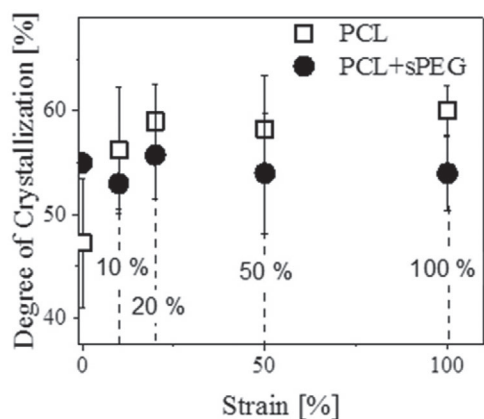


**Figure 5.** Degree of crystallization for PCL and PCL+sPEG-NCO fibers in dependence on the applied strain;  $n = 4$ . The crystallinity of pure PCL fibers increases with increasing strain, whereas it is constant with sPEG-NCO as additive.

Since necking is a crystallization process, this observation can be validated by determining the degree of crystallinity. Therefore, meshes which were pre-stretched to a defined strain ratio were characterized by XRD (Figure 5). While the degree of crystallization for the fibers with sPEG as additive was independent on the applied strain within the measurement error, the pure PCL fibers showed an increase of the crystallinity up to 20% strain. Although the crystallinity of the unstretched meshes is higher for fibers with sPEG-NCO as additive compared to PCL fibers. This could be due to the formation of a sPEG-NCO shell which can hinder the solvent evaporation and extend the solidification time hence increasing the crystallinity.<sup>[34]</sup>

## 4. Conclusions

Hydrophilization of electrospun fibers by polymer blending is a simple and straight-forward approach; understanding this process significantly enhances its versatility. From these results, we can conclude that irrespective of the polymer functionality, applied voltage or conductivity, it is the polymer blend miscibility as well as fast solvent evaporation which are necessary for surface segregation. Additionally, Flory–Huggins interaction parameter  $\chi$  allows us to predict the combination of blends which can lead to hydrophilic surfaces, on electrospinning rendering more matrix-additive systems accessible for the creation of hydrophilic fibers with functionality. The degree of surface segregation was determined by XPS which correlated to the Flory–Huggins interaction parameter. Furthermore, using sPEG-NCO as additive reduces fiber necking in blended fibers compared to pure PCL fibers. In addition to the hydrophilization and functionality, this renders the sPEG-NCO blended fibers an attractive candidate for tissue engineering application.

## Supporting Information

Supporting Information is available from the Wiley Online Library or from the author.

## Acknowledgements

The authors acknowledge support from the Leibniz Senate Competition Committee (SAW- 2015-DWI-2 471) under the Joint Initiative for Research and Innovation. This work was also supported by the Deutsche Forschungsgemeinschaft (DFG) in the framework of the priority program 2014 “Towards an Implantable Lung,” project numbers: 346972946 and 347367912 and was performed in part at the Center for Chemical Polymer Technology, supported by the EU and the state of North Rhine-Westphalia (Grant No. EFRE 30 00 883 02).

## Conflict of Interest

The authors declare no conflict of interest.

## Keywords

electrospinning, fiber necking, Flory–Huggins interaction parameter, hydrophilization, surface segregation

Received: August 23, 2019

Revised: September 16, 2019

Published online: October 17, 2019

- [1] D. Grafahrend, K. H. Heffels, M. V. Beer, P. Gasteier, M. Moller, G. Boehm, P. D. Dalton, J. Groll, *Nat. Mater.* **2011**, *10*, 67.
- [2] R.-Q. Kou, Z.-K. Xu, H.-T. Deng, Z.-M. Liu, P. Seta, Y. Xu, *Langmuir* **2003**, *19*, 6869.
- [3] M. P. Prabhakaran, J. R. Venugopal, C. Chan, S. Ramakrishna, *Nanotechnology* **2008**, *19*, 455102.
- [4] A. V. Bazilevsky, A. L. Yarin, C. M. Megaridis, *Langmuir* **2007**, *23*, 2311.
- [5] T. Croll, A. J. O'Connor, G. Stevens, J. Cooper-White, *Biomacromolecules* **2004**, *5*, 463.
- [6] R. Huang, H. Deng, T. Cai, Y. Zhan, X. Wang, X. Chen, A. Ji, X. Li, *J. Biomed. Nanotechnol.* **2014**, *10*, 1346.
- [7] K. Klinkhammer, N. Seiler, D. Grafahrend, J. Gerardo-Nava, J. Mey, G. A. Brook, M. Möller, P. D. Dalton, D. Klee, *Tissue Eng., Part C* **2009**, *15*, 77.
- [8] H. S. Yoo, T. G. Kim, T. G. Park, *Adv. Drug Delivery Rev.* **2009**, *61*, 1033.
- [9] S. J. Hardman, N. Muhamad-Sarih, H. J. Riggs, R. L. Thompson, J. Rigby, W. N. A. Bergius, L. R. Hutchings, *Macromolecules* **2011**, *44*, 6461.
- [10] J.-F. Zhang, D.-Z. Yang, F. Xu, Z.-P. Zhang, R.-X. Yin, J. Nie, *Macromolecules* **2009**, *42*, 5278.
- [11] R. L. Andersson, V. Ström, U. W. Gedde, P. E. Mallon, M. S. Hedenqvist, R. T. Olsson, *Sci. Rep.* **2014**, *4*, 6335.
- [12] L. A. Smith, P. X. Ma, *Colloids Surf., B* **2004**, *39*, 125.
- [13] A. Nishiguchi, S. Singh, M. Wessling, C. J. Kirkpatrick, M. Moller, *Biomacromolecules* **2017**, *18*, 719.
- [14] R. A. Neal, S. M. Lenz, T. Wang, D. Abeyayehu, B. P. C. Brooks, R. C. Ogle, E. A. Botchwey, *Nanomater. Environ.* **2014**, *2*, 1.
- [15] B.-M. Min, G. Lee, S. H. Kim, Y. S. Nam, T. S. Lee, W. H. Park, *Biomaterials* **2004**, *25*, 1289.
- [16] F. Yang, R. Murugan, S. Wang, S. Ramakrishna, *Biomaterials* **2005**, *26*, 2603.
- [17] H. Yoshimoto, Y. M. Shin, H. Terai, J. P. Vacanti, *Biomaterials* **2003**, *24*, 2077.
- [18] E. Zussman, D. Rittel, A. L. Yarin, *Appl. Phys. Lett.* **2003**, *82*, 3958.



- [19] E. D. Boland, J. A. Matthews, K. J. Pawlowski, D. G. Simpson, G. E. Wnek, G. L. Bowlin, *Front. Biosci.* **2004**, 9, 1422.
- [20] H. Yin, X.-H. Wang, X.-D. Zhu, H. Han, W.-Y. Guo, Z.-R. Fu, *J. Biomed. Nanotechnol.* **2013**, 9, 1345.
- [21] A. Rossi, L. Wistlich, K.-H. Heffels, H. Walles, J. Groll, *Adv. Healthcare Mater.* **2016**, 5, 1939.
- [22] T. K. Dash, V. B. Konkimalla, *J. Controlled Release* **2012**, 158, 15.
- [23] Y. Wang, G. A. Armeer, B. J. Sheppard, R. Langer, *Nat. Biotechnol.* **2002**, 20, 602.
- [24] K. G. Birukov, J. R. Jacobsen, A. A. Flores, S. Q. Ye, A. A. Birukova, A. D. Verin, J. C. N. Garcia, *Am. J. Physiol. Lung Cell. Mol. Physiol.* **2003**, 285, L785.
- [25] X. Y. Sun, R. Shankar, H. G. Börner, T. K. Ghosh, R. J. Spontak, *Adv. Mater.* **2007**, 19, 87.
- [26] X.-Y. Sun, L. R. Nobles, H. G. Börner, R. J. Spontak, *Macromol. Rapid Commun.* **2008**, 29, 1455.
- [27] G. Collins, J. Federici, Y. Imura, L. H. Catalani, *J. Appl. Phys.* **2012**, 111, 044701.
- [28] S. Koombhongse, W. Liu, D. H. Reneker, *J. Polym. Sci., Part B: Polym. Phys.* **2001**, 39, 2598.
- [29] G. Yazgan, R. I. Dmitriev, V. Tyagi, J. Jenkins, G. M. Rotaru, M. Rottmar, R. M. Rossi, C. Toncelli, D. B. Papkovsky, K. Maniura-Weber, G. Fortunato, *Sci. Rep.* **2017**, 7, 158.
- [30] B. A. Miller-Chou, J. L. Koenig, *Prog. Polym. Sci.* **2003**, 28, 1223.
- [31] M. M. Coleman, C. J. Serman, D. E. Bhagwagar, P. C. Painter, *Polymer* **1990**, 31, 1187.
- [32] H. H. Kim, M. J. Kim, S. J. Ryu, C. S. Ki, Y. H. Park, *Fiber Polym.* **2016**, 17, 1033.
- [33] C. T. Koh, D. G. Strange, K. Tonsomboon, M. L. Oyen, *Acta Biomater.* **2013**, 9, 7326.
- [34] A. S. Asran, M. Salama, C. Popescu, G. H. Michler, *Macromol. Symp.* **2010**, 294, 153.